Evidence for solar cycle influence on the infrared energy budget and radiative cooling of the thermosphere

Martin G. Mlynczak (*NASA Langley Research Center, Hampton, VA*)
F. Javier Martin-Torres (*AS & M, Inc., Hampton, VA*)
B. Thomas Marshall (*G & A Technical Software, Newport News, VA*)
R. Earl Thompson (*G & A Technical Software, Newport News, VA*)
Joshua Williams (*Utah State University, Logan, UT*)
Timothy Turpin (*Utah State University, Logan, UT*)
D. P. Kratz (*NASA Langley Research Center, Hampton, VA*)
James M. Russell (*Hampton University, Hampton, VA*)
Tom Woods (*LASP, Boulder, CO*)
Larry L. Gordley (*G & A Technical Software, Newport News, VA*)

Abstract. We present direct observational evidence for solar cycle influence on the infrared energy budget and radiative cooling of the thermosphere. By analyzing nearly five years of data from the Sounding of the Atmosphere using Broadband Emission Radiometry (SABER) instrument, we show that the annual mean infrared power radiated by the nitric oxide (NO) molecule at 5.3 μm has decreased by a factor of 2.9. This decrease is correlated (r = 0.96) with the decrease in the annual mean F10.7 solar index. Despite the sharp decrease in radiated power (which is equivalent to a decrease in the vertical integrated radiative cooling rate), the variability of the power as given in the standard deviation of the annual means remains approximately constant. A simple relationship is shown to exist between the infrared power radiated by NO and the F10.7 index, thus providing a fundamental relationship between solar activity and the thermospheric cooling rate for use in thermospheric models. The change in NO radiated power is also consistent with changes in absorbed ultraviolet radiation over the same time period.

1. Introduction

The primary radiative cooling mechanism in the terrestrial thermosphere is the infrared emission from the NO molecule at 5.3 μm [*Kockarts*, 1980]. Although the emission has been measured previously during suborbital rocket flights, global observations of this fundamental process were not available until the launch of the NASA Thermosphere-Ionosphere-Mesosphere Energetics and Dynamics (TIMED) satellite in December, 2001. The SABER instrument on the TIMED satellite continuously observes this emission at high vertical and horizontal resolution, enabling global characterization of the radiative cooling and its variability. SABER records approximately 1600 vertical profiles of NO limb radiance per day. Over 2.5 million radiance

profiles (encompassing approximately 1 billion individual limb radiance samples) are used in this analysis.

Since the TIMED launch, a focus of the analyses of the SABER NO emission data has been on the "natural thermostat" effect of nitric oxide in response to intense geomagnetic storms caused by coronal mass ejections [*Mlynczak et al*., 2003; 2005]. These analyses laid the groundwork for understanding the role infrared radiation plays in allowing the thermosphere to rapidly recover from perturbations caused by geomagnetic disturbances. In this paper we apply the same analysis techniques as in the *Mlynczak et al*. papers cited above, but to the entire SABER dataset now nearing five years in length. The analysis reveals a remarkable decrease in radiated power from the thermosphere during this time, a decrease that is strongly correlated with the decrease in the solar 10.7 cm radio flux as indicated by the F10.7 index. This correlation strongly implies the decrease in radiated NO power is associated with the declining activity of the present solar cycle.

In Section 2 we review the analysis procedure used to derive the daily global radiated power from NO at 5.3 μm, starting with the measured SABER limb radiances. In Section 3 we present the results of this analysis, on a year-by-year basis, including the running annual means. The results are discussed in Section 3 wherein simple relationship between the annual mean F10.7 index and the annual mean NO power is given. Analysis of the results is given in Section 4, followed by a comparison with the solar input variability in Section 5. The paper concludes with a summary section.

2. Analysis Technique

In this paper we follow the analysis technique given in *Mlynczak et al*. [2005] as amended by *Mlynczak et al*. [2006]. For each day we derive the global average power radiated by

the NO molecule as derived from SABER limb radiance measurements. The essential steps of this technique are reviewed here.

First, an Abel inversion is applied to the SABER-measured limb radiance (W m^{-2} sr^{-1}) to yield a volume emission rate (W m^{-3}) of energy. The Abel inversion is valid because the radiative transfer is in the weak-line limit. However, because SABER is a filter radiometer, the volume emission rate derived in this step is not representative of the total rate of emission from the NO molecule. Rather, it is a measure of the total emission as weighted by the relative spectral response function of the SABER instrument. An "unfilter" correction factor, presently derived from theory, is applied to this in-band emission rate to obtain the total emission rate from the NO molecule. *Gardner et al*. [2006] have independently derived the unfilter factor by analyzing NO spectra recorded by the MIPAS instrument on the EnviSat satellite. Their values agree well with the theoretical values used in the operational SABER data processing.

The next step after deriving the total NO emission rate in W m^{-3} is to vertically integrate this rate to obtain the flux (W m^{-2}) of energy out of the thermosphere. All of the radiation emitted by NO escapes the thermosphere; one-half of it exits to space, the other is absorbed in the lower atmosphere. The altitude range of the vertical integration is 100 km to 200 km. The fluxes are sorted into 5 degree bins of latitude, from which the power emitted within each latitude bin is obtained by multiplying the zonal mean flux within each bin by the area of the bin. This yields the power (W) radiated every 5 degrees in latitude. The next-to-final step in the process is to add up the power from each 5 degree latitude bin to obtain the total power radiated by the NO molecule.

The last step in the process is to recognize that due to the SABER viewing geometry on the TIMED spacecraft, the range of latitudes observed covers from 83 degrees in one hemisphere

to 55 degrees in the other. This range encompasses approximately 91% of the global atmospheric area; however, it does leave out one of the polar regions. Every 60 days the TIMED spacecraft yaws 180 degrees, enabling SABER to change its hemispherical latitude coverage. To estimate the total power radiated by the entire atmosphere (pole to pole), we assume that the ratio of the power emitted between the equator and 55 degrees latitude to the power emitted from 55 degrees to the pole is the same in both hemispheres. This provides an estimate of the power emitted by the entire atmosphere.

3. Results

The process above was followed by *Mlynczak et al.* [2005] to analyze the ten days in April, 2002 during which a very strong geomagnetic disturbance occurred accompanied by a large increase in the strength of the NO emission from the thermosphere. This process is now applied to the entire SABER dataset. Shown in Figure 1 are five frames of data showing the daily global power radiated by NO from 2002 (when routine mission operations began) through 2006. The feature that is most readily apparent in the data is the variability of the daily NO power. Also readily apparent are the major storm events such as the "Halloween Superstorms" shortly after day 300 in 2003, and again after day 310 in 2004, when the daily global power emitted by NO exceeded 1 terawatt. The events studied in detail by *Mlynczak et al*. [2005] correspond to the enhanced power at day 110 in 2002. Upon closer inspection of the data in Figure 1 it is clear that the overall level of radiated power by NO has decreased from 2002 to 2006. To more clearly illustrate the overall temporal variation and decrease of the daily power we plot in Figure 2 on a logarithmic scale the data from Figure 1 as one continuous time series. It is evident that the NO power has been steadily decreasing since the start of the mission, although the signal is quite variable.

The decrease in NO power over time can be clearly seen if we compute the running annual means of the NO power. Starting at day 25 in 2002 (the first fully operational day), we compute the annual mean for the next 365 days of data. We do this again for day 26, and so on for each consecutive day, obtaining over 1300 values of the annual running mean. Days in which there is little or no SABER data are not included; typically this is no more than five to eight days in any 365 day window. The period of one year is chosen so that the average is computed for an integral number of spacecraft yaw cycles, six in the case of the TIMED satellite.

In Figure 3 we show with the solid curve the running annual mean computed from the start of the mission. The abscissa indicates the first day of the 365 for which the mean is computed. In this sense the means can be interpreted as "forward" running means starting from the indicated day. The dashed curve in this figure is the standard deviation of the annual means, again in the "forward" sense. Clearly evident is a decrease in the NO power from the start of the mission, by a factor of approximately 2.9. Despite this large decrease, the standard deviation remains essentially constant over this time. The observed increase in the standard deviation at day 300 is a direct consequence of the forward running mean now including the "Halloween superstorm" of October 2003. Similarly, the decrease in the standard deviation after day 1000 is a consequence of the running mean no longer including the terawatt event near day 315 in 2004 (see Figure 1).

The observed decrease in the NO power occurs during the declining phase of the present solar cycle. Over the same time period covered in Figure 3, the annual running mean F10.7 index decreases monotonically from 175 to 83. Shown in Figure 4 is a plot of the running annual mean NO power derived from SABER measurements against the running annual mean F10.7 solar

index. The linear correlation coefficient for these data is 0.96. The solid curve in Figure 4 represents a second-order polynomial fit to the data. Specifically,

$$P = a_0 + a_1 F + a_2 F^2 \quad (1)$$

where P is the annual running mean (again, forward one year from a given date), F is the annual running mean F10.7 index (again, forward one year from a given date), and a_0, a_1, and a_2 are equal to –3.85, 7.51 x 10^{-2}, and -2.18 x 10^{-4}, respectively. Equation 1 provides a fundamental relationship between solar variability and the dominant term in the infrared energy balance of the entire thermosphere. It also provides a fundamental empirical constraint that can be used in testing numerical models of the thermosphere, in the sense that the annual power computed in a model run of one year or longer can be compared with the F10.7 index values which are often used to parameterize the solar variability in the models.

4. Analysis

To understand the reasons for the variability in the NO radiated power, it is instructive to consider the expression for the flux (F, W m^{-2}) radiated by NO at a specific latitude and longitude. Recall that the volume emission rate derived by SABER is the volume emission rate (W m^{-3}) of energy which is directly related to the radiative cooling rate through the first law of thermodynamics. Specifically, we can write (to first order) from the definition of the flux and the first law:

$$F = \int_z V(z)\,dz = \int_z \rho(z) C_p \frac{\partial T(z)}{\partial t} dz \quad (2)$$

where V(z) is the SABER-derived volume emission rate, ρ(z) is the density, C_p is the heat capacity at constant pressure, and $\partial T(z)/\partial t$ is the rate of radiative cooling (K day^{-1}). Thus, the flux, and hence the global power presented above, represents the density-weighted, vertically

integrated radiative cooling rate of the thermosphere. The observed decrease in the flux and power radiated by NO directly implies a decrease in the radiative cooling of the thermosphere that is coincident with the decline in activity in the current solar cycle.

To further interpret the observed decrease in radiated power, to first order we can write the flux *F* as:

$$F = E_{10}\, A_{10}\, k_{10}\, g_0 \int_z \frac{[NO(z)]}{Q(z)}\,[O(z)]\,\frac{\exp[-E_{10}/k_B T(z)]}{A_{10} + k_{10}\,[O(z)]}\,dz \qquad (3)$$

Equation (3) is derived from a vertical integration of the volume emission rate, assuming a two vibrational level NO molecule, i.e., a ground state and a first excited state for NO. Only spontaneous emission of radiation from the first excited state and collisional excitation and quenching (by collisions with atomic oxygen) of ground and excited state are considered for this illustration. In Equation (3) NO(z) and O(z) are the concentrations of nitric oxide and atomic oxygen at altitude z, respectively, A_{10} is the lifetime against spontaneous emission of the first excited NO vibrational level, k_{10} is the rate coefficient for quenching of the first excited state of NO in collisions with atomic oxygen, E_{10} is the energy of the first excited state above ground, k_B is Boltzmann's constant, Q(z) is the vibrational partition function for NO, g_0 is the degeneracy of the ground state, and T(z) is the kinetic temperature at altitude z. We note that k_{10}, being independent of temperature [*Hwang et al*., 2003], is effectively constant with altitude.

Upon inspection of Equation (3) it is evident that the flux (and hence the radiated power) depends linearly on the NO density, at most linearly on the atomic oxygen density, and non-linearly on temperature. We would expect all three quantities (NO, O, and T) to decrease during the declining phase of a solar cycle because less ultraviolet radiation enters the thermosphere from the Sun. The extent to which the relative variability of these three factors individually influences the variability of the radiated power remains to be quantitatively determined.

Some insight is gained into the importance of the variability of the NO density by examining the correlation between the NO power and the NO column density, the latter as observed by the HALOE instrument (from the lower stratosphere into the lower thermosphere) that operated on the UARS satellite through 2005. Due to sampling issues, the latitude range of the HALOE data for this purpose is ± 45 deg. Within these parameters, there are about 490 days in which both HALOE and SABER were operational before the UARS mission was ended in 2005. The linear correlation coefficient between the lower thermospheric (105 to 140 km) column NO derived from HALOE and the power derived from SABER is found to be 0.59, when taking the NO power between ± 55 degrees latitude, the latitude range continuously observed by SABER. The relatively low correlation coefficient, for these latitudes at least, suggests that variations in NO density alone are not adequate to account for the observed variations in NO infrared radiated power. This then suggests that NO variations together with temperature and atomic oxygen variations are jointly responsible for the observed changes.

5. Consistency with Changes in Solar Energy Output

From the annual mean NO power presented above we can compute the change in the outgoing longwave radiation from the thermosphere from the start of the TIMED mission. Using the data presented above, the change in the running annual mean power from Day 39 2002 until Day 199 2005 is found to be 1.65×10^{11} W (165 GW). We can compare this with the change in solar output by comparing with the change in ultraviolet radiation measured by the Solar EUV Experiment (SEE) on TIMED [*Woods et al*., 2005] and by the Solar Radiation and Climate Experiment (SORCE) [*Rottman*, 2005].

We first consider the change in the absorbed UV radiation in the Schumann-Runge Continuum (SRC). The cross sections in this band are independent of temperature and pressure. Thus the global absorbed power *P* is estimated by:

$$P = \pi r_{eff}^2 \sum_{\lambda} F_{\lambda}^{o} (1 - \exp(-\sigma_{\lambda} u)) \quad (5)$$

where *P* is the global absorbed power (W), F_{λ}^{o} is the exoatmospheric solar irradiance (W m^{-2} nm^{-1}, from SEE and SORCE), σ_{λ} is the SRC cross section (cm^2) at wavelength λ, and u is the optical mass (cm^{-2}). To estimate the global power we use an optical mass of molecular oxygen (O_2) above 100 km of 2 x 10^{18} cm^{-2} based on a vertical optical mass of 1 x 10^{18} cm^2 and a global mean solar zenith angle of 60 degrees. The term r_{eff} is the effective radius of the Earth's disk that absorbs the UV radiation, which we take to be 6520 km, or 150 km larger than the average Earth radius. The summation is carried out in 1 nm bins from 130.5 nm to 173.5 nm. The Lyman-α line at 121.5 nm is included in addition to the SRC and adds a few percent to the sum.

SORCE was launched in early 2003 and data are available from 25 January 2003. In comparisons with the SEE data an offset between the two datasets of about 8% was observed, with the SEE SRC being larger. To construct a continuous solar irradiance dataset from the start of the TIMED mission we combine SEE data (scaled down by a factor of 1.08) from January 2002 until January 2003, and then use SORCE data from that point forward. The SORCE data are believed to be more accurate than the SEE data at this point in time.

Using this blended set of solar irradiance data, we compute *P* as defined above for each day and then evaluate the annual running mean in the same way as for the NO power from SABER. Shown in Figure 5 is the daily absorbed power estimated according to Eq. (5) and the corresponding daily running mean power (dashed curve). Although the archived SEE and

SORCE data are nominally at 1 AU, we have adjusted them to reflect the actual Earth-Sun distance.

From these data we determine that the change in absorbed UV in the SRC over the same extent of time as the SABER NO data is 2.05 x 10^{11} W or 205 GW. The majority of the absorbed energy in the SRC in fact goes into chemical potential energy of atomic oxygen which is realized as heat only long after the time of photon deposition, as the O is transported downward to an altitude where density is sufficient for recombination to occur. Thus the difference between the NO power and the SRC is perhaps not surprising – the majority of the energy absorbed in the SRC is likely not liberated in the thermosphere.

There are of course several other important terms in the energy budget of the thermosphere. All solar radiation shorter than 120 nm is absorbed in the thermosphere, and Joule and particle heating are important. *Knipp et al*. [2005] note changes of 203 GW in solar radiation below 120 nm and 35 GW in Joule heating from solar maximum to solar minimum. Cooling due to emission from CO_2 at 15 μm and atomic oxygen at 63 μm must also be considered in any detailed assessment of the overall energy budget, and will be the subject of a subsequent paper. Nevertheless, the change in NO emission over the course of the TIMED mission to date appears to be consistent with the changes in solar radiation considering the other terms in the balance yet to be evaluated.

6. Summary and Conclusions

We have analyzed nearly five years of measurements of infrared emission from NO made by the SABER instrument on the TIMED satellite. SABER limb radiance measurements are inverted to yield vertical profiles of the volume emission rate of energy from the NO molecule. The emission rates are then used to derive the daily global power radiated by the NO molecule

from the thermosphere between 100 and 200 km altitude. The data exhibit significant day-to-day variability. Over the period of extant data, the daily NO power is observed to decrease significantly. The observed decrease in radiated power is directly related to a decrease in the radiative cooling rate of the thermosphere The annual running mean power decreases by a factor of 2.9, and is strongly correlated with the decrease in the annual running mean value of the F10.7 solar index, implying that the observed decrease in NO power (and radiative cooling rate) is caused by the decline in solar activity. The variance of the annual means remains essentially constant and is visibly influenced by the occurrence of major storm events (i.e., those in which the daily power radiated by NO is found to exceed one terawatt.) The magnitude of the change in NO emission appears consistent with that expected from changes in solar inputs.

The last day of NO data used in the analysis above was day 238 of 2006. The NO power data through this date (i.e., Figures 1 and 2) do not yet exhibit evidence to confirm that solar minimum has been reached. It is anticipated that the NO power will increase as the Sun passes through the minimum of the current 11-year cycle and begins building up to the next maximum. The database of NO power will be continually updated as the TIMED mission goes on for the next several years. The database of NO power presented here, which also includes values of the A_p, K_p, and F10.7 indexes, is available from the first author of this paper at the e-mail address given below. These data should prove valuable in studying the relative roles of natural and anthropogenic change in the thermosphere.

Acknowledgement. The authors would like to thank the NASA Science Mission Directorate for continued support of the TIMED mission and the SABER project. MGM would like to thank the NASA Langley Science Directorate for continued support.

(Martin G. Mlynczak, NASA Langley Research Center, Mail Stop 420, Hampton, VA, 23681. m.g.mlynczak@nasa.gov)

References

Gardner, J., et al., Comparison of nighttime NO 5.3 μm emissions in the thermosphere measured by MIPAS and SABER, *J. Geophys. Res*., submitted, 2006.

Hwang E. S., K. J. Castle, and J. A. Dodd, Vibrational relaxation of NO(v = 1) by oxygen atoms between 295 and 825 K, *J. Geophys. Res*., 108 (A3), 1109, doi:10.1029/2002JA009688, 2003.

Knipp, D. J., W. K. Tobiska, and B. A. Emery, Direct and indirect thermospheric heating sources for solar cycles 21-23, Solar Physics, 224, 495-505, doi:10.1007/s11207-005-6393-4, 2005.

Kockarts, G., Nitric oxide cooling in the terrestrial thermosphere, *Geophys. Res. Lett*., 7, 137-140, 1980.

Mlynczak, M. G., et al., Correction to "Energy transport in the thermosphere during the solar storms of April, 2002, *J. Geophys. Res*., *submitted*, 2006.

Mlynczak M. G., et al., Energy transport in the thermosphere during the solar storms of April 2002, *J. Geophys. Res*., 110, A12S25, doi:10.1029/2005JA011141, 2005.

Mlynczak M. G., et al., The natural thermostat of nitric oxide emission at 5.3 μm in the thermosphere observed during the solar storms of April 2002, *Geophys. Res. Lett*., 30 (21), 2100, doi:10.1029/2003GL017693, 2003.

Rottman, G., The SORCE Mission, Solar Physics, 230, 7-25, 2005.

Woods T. N., et al., Solar EUV Experiment (SEE): Mission overview and first results, *J. Geophys. Res*., 110, A01312, doi:10.1029/2004JA010765, 2005.

Figure Captions

Figure 1. Daily global power (W) radiated by NO from 2002 to 2006.

Figure 2. Time series of daily global NO power from 2002 to 2006 on a logarithmic scale.

Figure 3. Running annual mean of the daily global NO power from Figure 2 (solid curve) and the corresponding standard deviation of the running mean (dashed curve).

Figure 4. Running annual mean of the global NO power plotted against the running mean of the F10.7 solar index (diamonds). The solid curve is the equation fit to the data described by Equation 2.

Figure 5. Absorbed power (Terawatts) in the Schumann-Runge Continuum based on SEE and SORCE data. Daily power is indicated by the solid curve and the annual mean power is in the dashed curve.

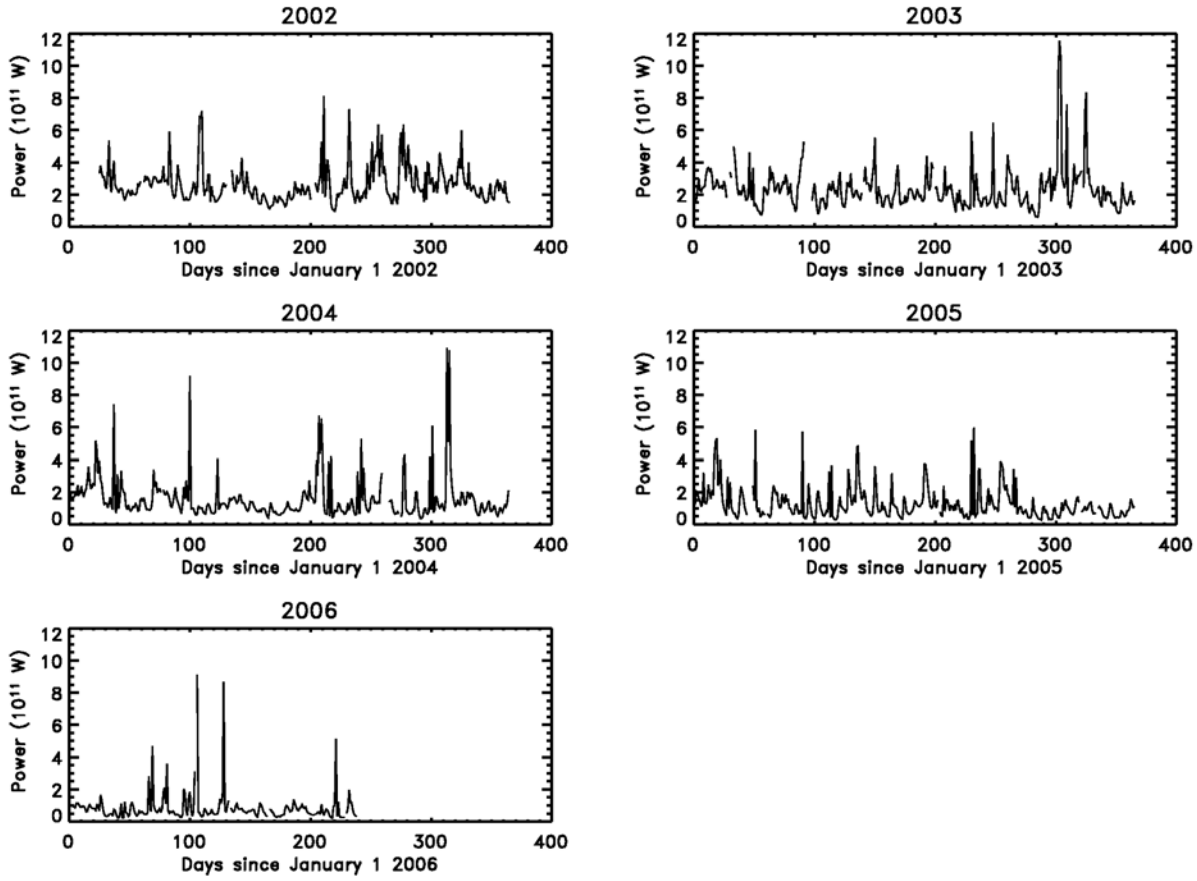

Figure 1. Daily global power (W) radiated by NO from 2002 to 2006.

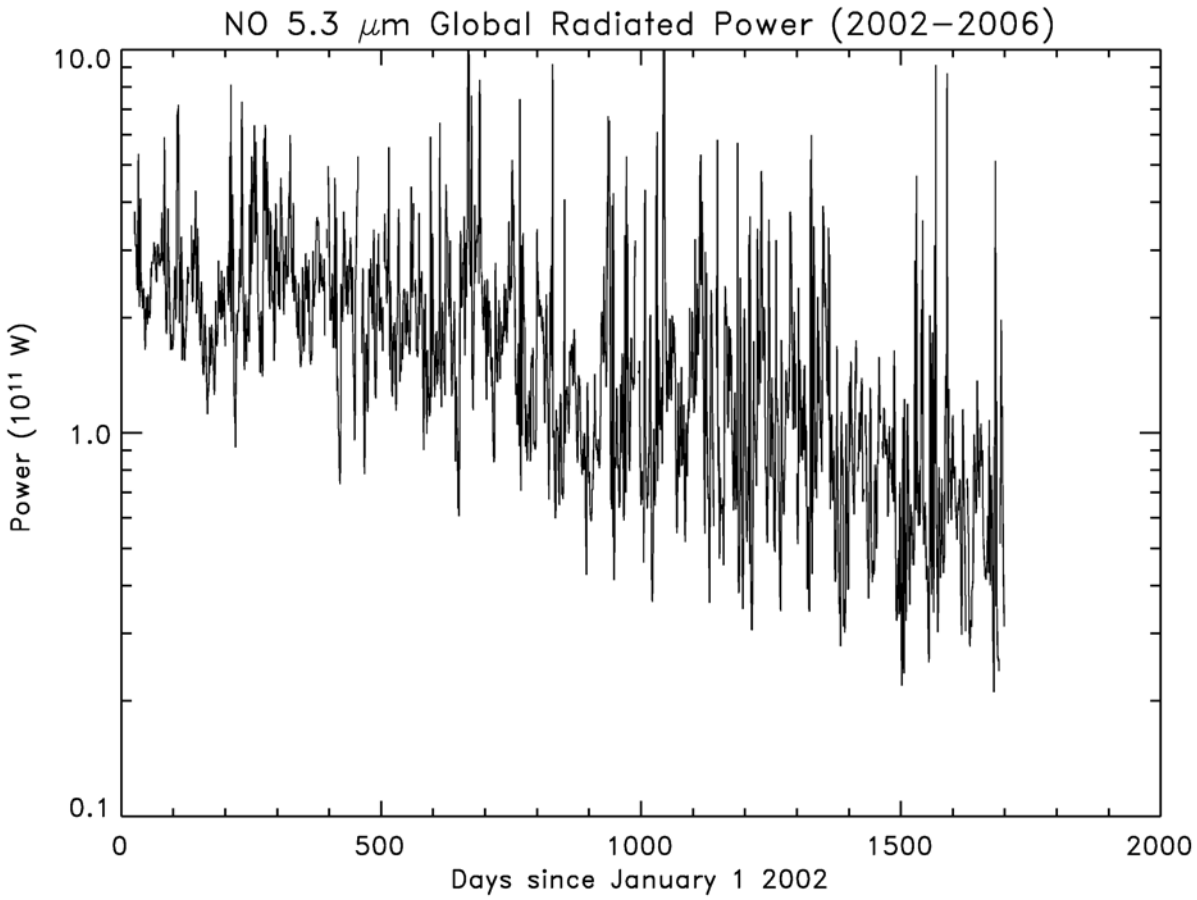

Figure 2. Time series of daily global NO power from 2002 to 2006 on a logarithmic scale.

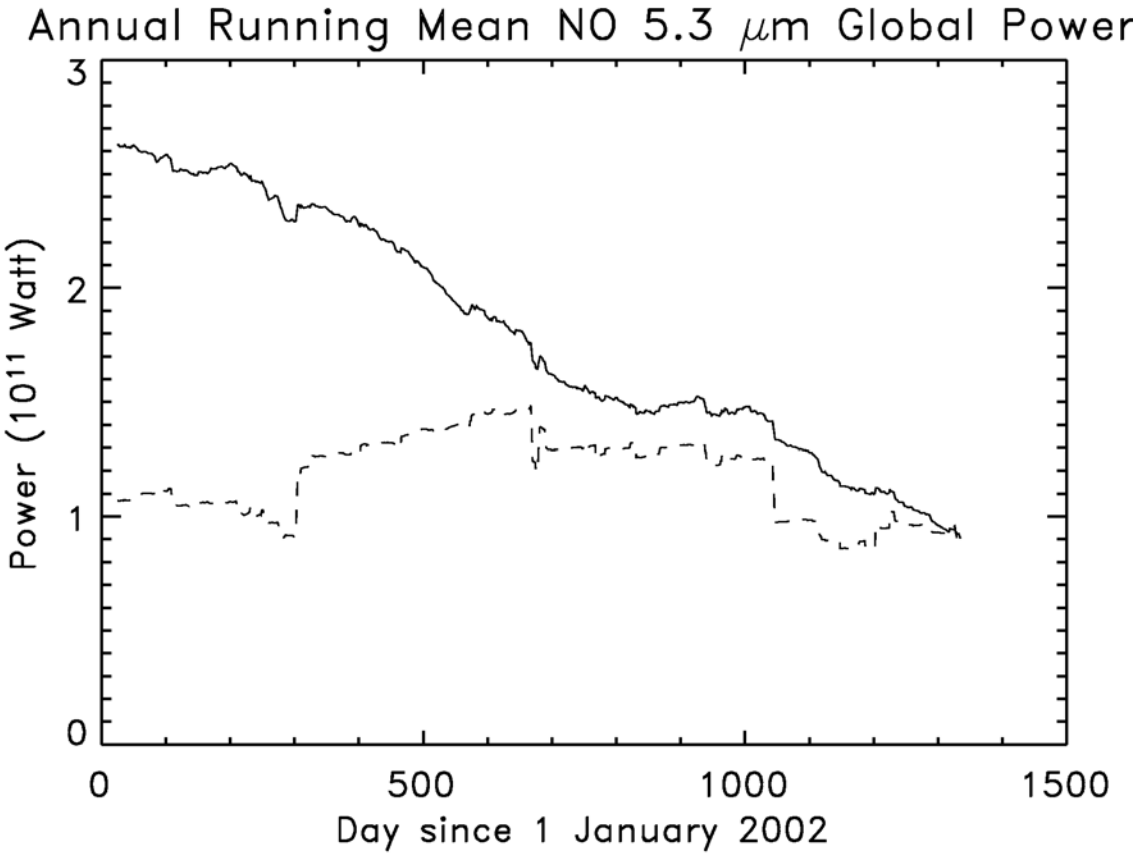

Figure 3. Running annual mean of the daily global NO power from Figure 2 (solid curve) and the corresponding standard deviation of the running mean (dashed curve).

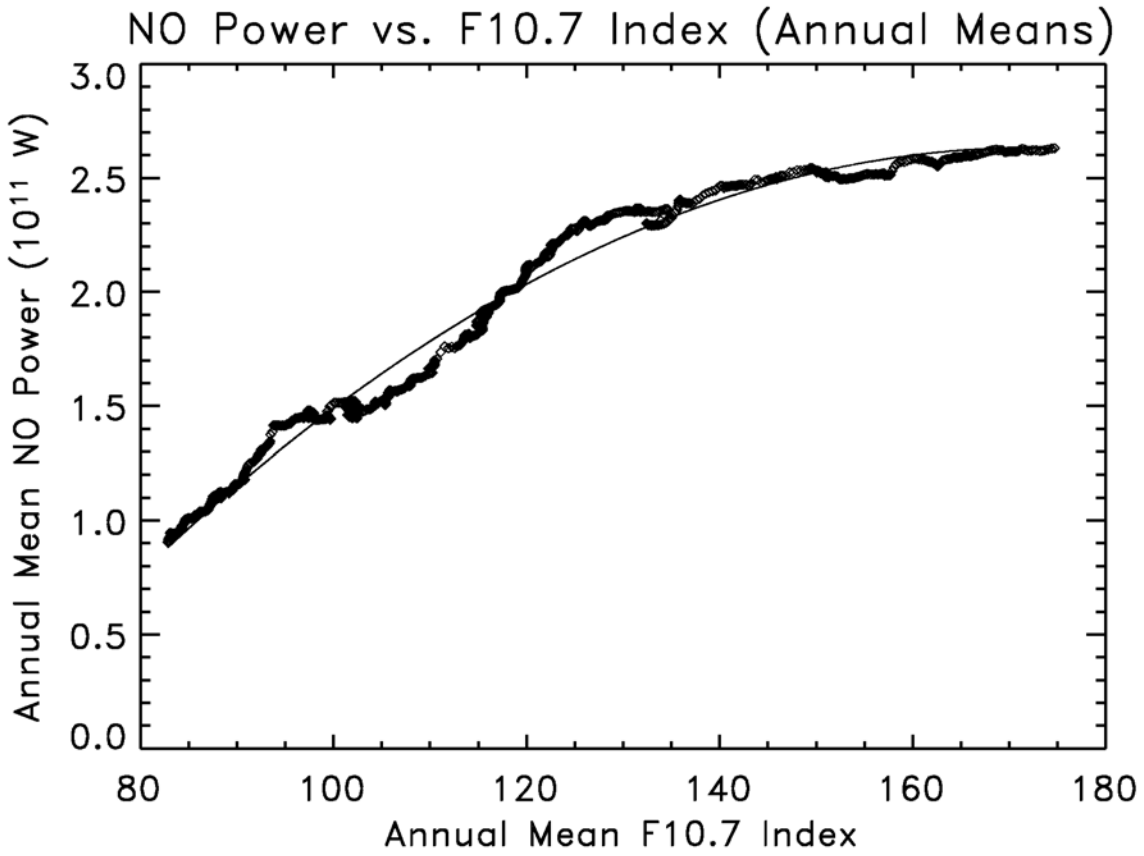

Figure 4. Running annual mean of the global NO power plotted against the running mean of the F10.7 solar index (diamonds). The solid curve is the equation fit to the data described by Equation 2.

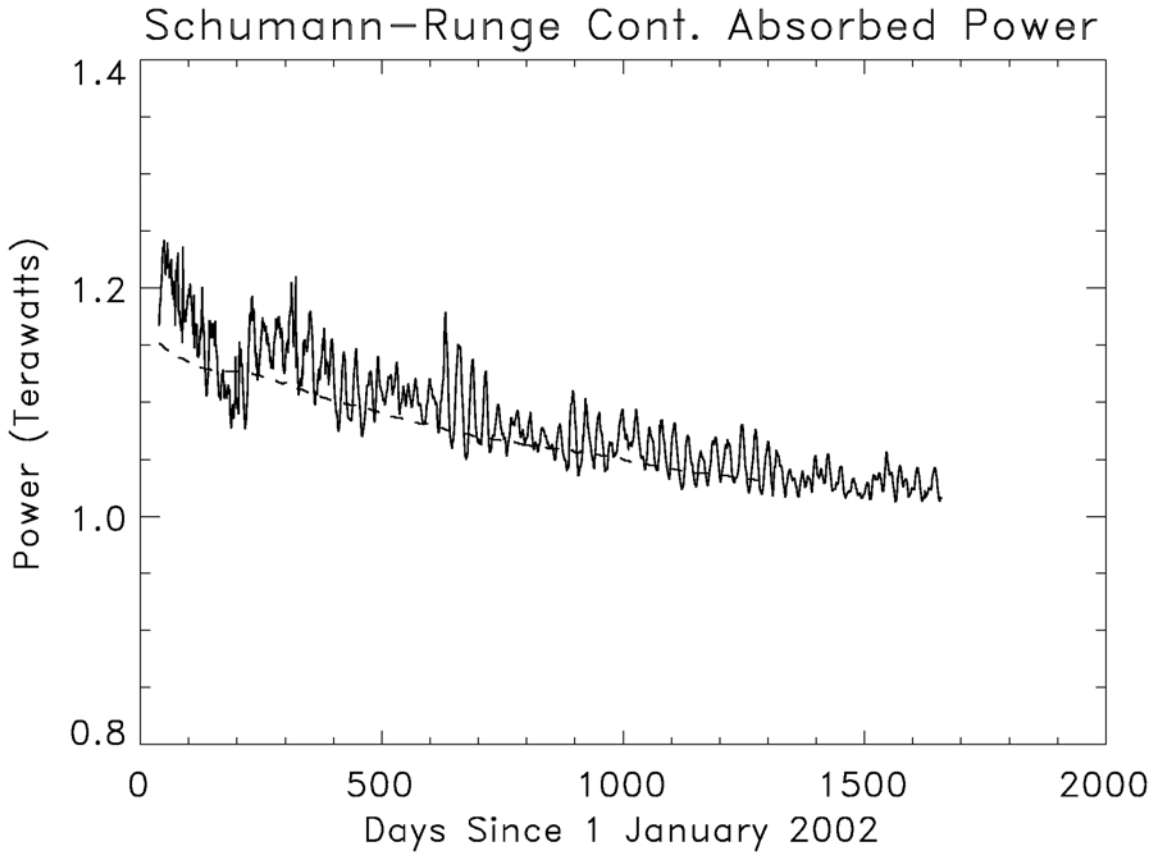

Figure 5. Absorbed power (Terawatts) in the Schumann-Runge Continuum based on SEE and SORCE data. Daily power is indicated by the solid curve and the annual mean power is in the dashed curve.